

# 10

## Aggregate behavior in zooplankton: Phototactic swarming in four developmental stages of *Coullana canadensis* (Copepoda, Harpacticoida)

JEANNETTE YEN AND ELIZABETH A. BUNDOCK

### 10.1 Introduction

#### 10.1.1 Zooplankton swarming

Uneven distributions of zooplankton, where concentrations can be two to three orders of magnitude greater than the average abundance, have been well documented (Ambler et al. 1991; Omori & Hamner 1982; Ueda et al. 1983; Wishner et al. 1988). Such aggregations have been considered mandatory for the survival of plankton that need to feed at high food concentrations to meet their metabolic costs (Davis et al. 1991; Lasker 1975). In attempting to quantify zooplankton patchiness, researchers have surveyed patch size and density on a broad scale (Haury & Wiebe 1982; Wiebe et al. 1985) and examined the causes of patch formation and maintenance against the forces of mixing (Okubo & Anderson 1984). Within patches, research has focused on genetic relatedness (Bucklin 1991) and physiological limitation (fish – McFarland & Okubo Ch. 19; krill – Morin et al. 1989). However, a measure of zooplankton patchiness has challenged oceanographers for years (Hamner 1988). Average densities generally underestimate local densities because conventional sampling methods, such as net sampling, can pass through several swarms (Omori & Hamner 1982). This has led to the development of new methods for assessing the true abundance and distribution of zooplankton, including SCUBA, submersibles, video-imaging, acoustics, and optical counters (Alldredge et al. 1984; Schultze et al. 1992; Smith et al. 1992; Greene & Wiebe Ch. 4). Even with these newer techniques, it is difficult to monitor patch characteristics and dynamics because patches occur over a wide range of scales (Dickey 1990; Haury et al. 1978). There appears to be no single model of aggregation, in part because structuring factors are related to the scale of the patch: The broad scale is dominated by physics, the intermediate scale by group behavior, and the fine scale by individual responses (S. Levin, comment).

### **10.1.2 Mechanism and cues**

Zooplankton aggregation appears to be influenced by a variety of factors. Plankters can be passively concentrated or actively motivated. Passive aggregations can be produced by physical features of water motion, like eddies, fronts, shear layers, or Langmuir cells (Haury et al. 1978; Okubo 1984) which can restrict dispersion by currents. However, shear layers also can stimulate an active avoidance response (Haury et al. 1980; Yen & Fields 1992). Some zooplankton actively change their swimming behavior in response to food patches or odors (attractants – Hamner & Hamner 1977; Katona 1973; Poulet & Ouellet 1982; or deterrents – Folt & Goldman 1981), e.g. they swim shorter reaches and turn more frequently inside favorable patches compared to their behavior outside of patches (Price 1989; Tiselius et al. 1993; Williamson 1981). Others actively respond to light gradients (horizontal migrators follow certain angular light distributions – Siebeck 1969; Ringelberg 1969) or point sources (swarms form in light shafts – Ambler et al. 1991), or avoid water of certain temperatures or salinities (Wishner et al. 1988).

Each cue (e.g. light, odors, fluid motion) has a range of attributes, varying in time and space, such as

1. spectral quality or directionality of polarized light,
2. composition, age, or cohesiveness of chemical metabolites,
3. intensity (speed) and direction of water movement.

The signals must be discerned above the ambient noise of the aquatic environment. These are the external variables which lead the zooplankter to the swarm. Internally, variations in receptor sensitivities and physiological state of the organism will modulate their response to each cue, affecting whether they will join and stay in a swarm or leave it. Such cues change random-walk movement patterns into directed swimming paths (see Romey Ch. 12 for a discussion on whirligig beetle movement).

Phototaxis is a directional response to a light stimulus (Forward 1976). Given a defined light source, positively phototactic animals will be attracted and aggregations will form. For instance, Ambler et al. (1991) documented phototactic swarm formation of copepods to light shafts within mangrove prop roots. Although they note that light may be the proximal cue for swarm formation, predator avoidance is invoked as the ultimate cue. Light shafts are formed in between the shadows cast by interlacing prop roots. Thus, those copepods orienting to the light cue aggregated within the protection of the roots and away from open-water predatory fish. While phototaxis may be a proximal cue leading to copepod aggregation, swarm members must derive some ultimate benefits,

such as predator mediation or enhanced frequency of mating encounters (Hebert et al. 1980), in order for swarms to persist (see Hammer & Parrish Ch. 11).

Copepods are small (1–10 mm) crustaceans often found in large aggregations (1–10s of meters). Although a detailed study of swarming behavior in copepods is needed, this has yet to be done principally because of both logistical and analytical limitations. Fish schools are easy to detect and observe relative to copepod swarms. We still cannot stroll through the ocean as we do through forests to see midge swarms, although this is becoming more possible with the use of submersibles or remotely operated vehicles (ROV) equipped with cameras. Repeated sampling of patches is difficult since patches often do not occur in a reliable location and zooplankton can be easily disturbed. It has been difficult to monitor situations where we can evaluate quantitatively the individual-based dynamics of aggregative behavior. Furthermore, copepod movement patterns do not appear to be coordinated at the group level. Rather than forming regular arrays, such as those exhibited by polarized schools of fish, individual plankters move apparently haphazardly through the swarm.

Instead of attempting to perform in situ studies of zooplankton swarms, we now present results from a laboratory-induced copepod swarm. Thus, we can stimulate swarming behavior at a specified location by the phototactic response to a point source of light. When the light source is placed at the focal point of two videocameras oriented at right angles to each other, we can reconstruct the three-dimensional spatial locations in time ( $x, y, z, t$ ) of the swarmers from the two right-angle views. With such a laboratory-controlled situation, we can examine how copepods interact in close proximity to each other – as in a natural swarm. We began with analyses of the characteristics and kinematics of swarming: rate of aggregation and dispersion, patch size and density, trajectories, velocity of individuals, swimming patterns. Other behavioral patterns that presently are being examined include orientation, posture, and turning frequency.

## 10.2 Methods

*Coullana canadensis* is a harpacticoid copepod that is planktonic as a larva and epibenthic as an adult (Lonsdale & Levinton 1985). Each of four stages were separated from cultures of a population collected in Maine, that had been maintained in the laboratory for several generations. Stages were delimited by size: early nauplii (EN) 0.10–0.14 mm, late nauplii (LN) 0.16–0.26 mm, copepodids (COP) 0.28–0.60 mm, and adults (AD) 0.64–0.86 mm. Because nauplii are naturally found in the water column, they were used to examine swarm characteris-

tics. All stages were used in a behavioral analysis of locomotory patterns mechanically responsible for swarm formation and maintenance.

Prior to each experiment, selected copepods of each size/stage category were taken from the cultures and kept in filtered seawater for less than 12 h at room temperature (approximately 20°C). The copepods then were transferred to a small glass tank (5 cm<sup>3</sup>) filled with approximately 100 ml of filtered seawater. A 2-mm-diameter fiber optics light source suspended 3 cm off the bottom of the tank was used as the attractant stimulus. After a dark-acclimation period of 30 min, the copepods were subjected to a 10-min period of illumination followed by a 4-min period of darkness. Each stage was videotaped twice, on separate days, using different individuals. The density of animals in the tank, and thus available for patch formation, was either 50 or 200. The size of the swarm was smaller (< 5 mm in diameter) than the width of the tank (5 cm in width).

#### *Swarm visualization*

By duplicating the laser-illuminated videoimaging techniques of Strickler (1985), we developed a system to observe zooplankton swarms in three dimensions and record their behavior (Yen & Fields 1992). Two videocameras (Pulnix TM745 B/W high-resolution cameras), oriented at right angles to each other, were focused on the fiber optics light source positioned in the center of the square glass tank of seawater with copepods (Fig. 10.1). A HeNe laser light source, following a modified Schlieren optical light path, provided the illumination for the cameras; animals did not appear to be sensitive to this wavelength (632 nm) of light. Each camera recorded the activity within an area (10 mm × 15 mm) surrounding the light source on VHS-format tape at 30 frames/sec, magnifying the image 20 times. The magnification was adjusted so that as much of the swarm as possible was within the fields of view.

#### *Quantitative analysis*

The number of individuals that could be counted was limited by the camera's field of view and swarm size. At a density of 200 animals, copepods between the light and the camera but not within the focal plane appeared as double images. If the entire swarm was not in focus, many blurred images would appear on the screen. Because neither of these artifacts happened with a tank density of 50 animals, we assumed that the entire swarm was seen, even though swarm size was always less than 100% of the animals present in the tank. To estimate swarm size, the maximum number of copepods seen during a one-second interval (i.e. over 30 frames) was recorded every 5 sec during the first minute, every 10 sec during the second minute, and every 30 sec until the light was turned off. Select-

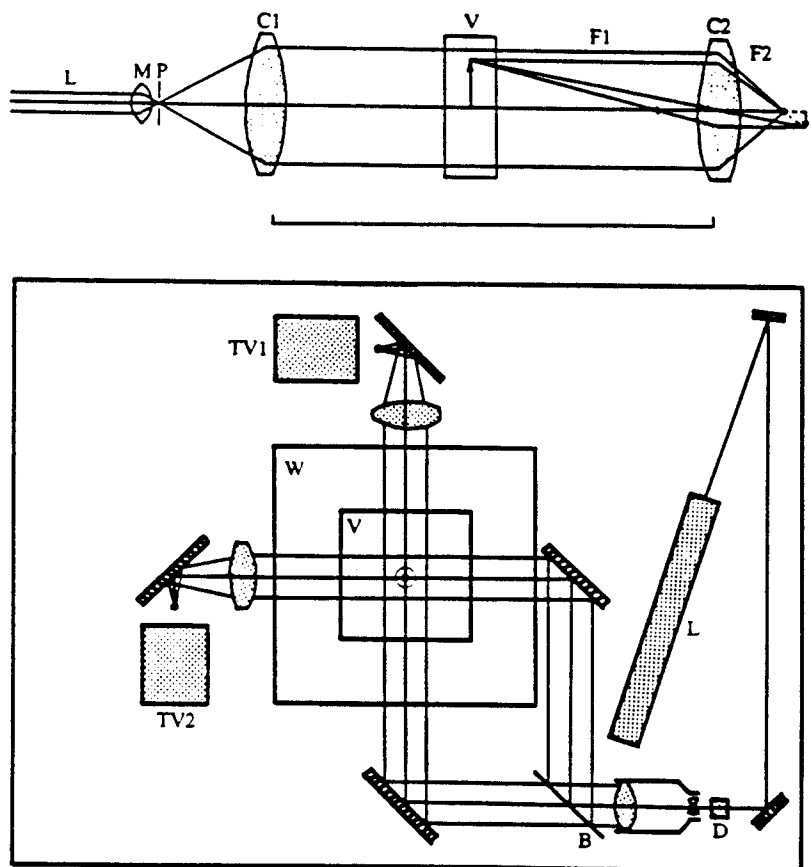


Figure 10.1. Diagram of optical pathway (Fig. 3 from Strickler 1985) and experimental setup (Fig. 5 from Strickler 1985) used to observe copepod swarms forming in the center of the vessel. Our setup is fixed frame and differs from the movable one shown here.

ing the maximum number within a one-second interval took the constant exchange of animals in and out of the swarm into account.

#### *Patch characteristics*

Patch dimensions and the percentage of available population in the swarm were examined for two densities of early nauplii: 50 and 200. Because the swarm appeared symmetric in both right-angle views, we analyzed patch characteristics from the two-dimensional projection of a single camera. After the swarm formed, the positions of the nauplii were digitized from a series of 20 frames. Concentric circles with centers at the light were placed over the plot. The density

of animals (#/vol) within a column below the light source at different distances from the light source was used to obtain an estimate of patch size.

To obtain three-dimensional ( $x, y, z$ ) coordinates with multiple two-dimensional projections of a swarm, it was necessary to match individuals viewed in one projection with individuals in the companion projection (see Osborn Ch. 3; Fig. 10.2). Initial analysis began with an examination of the two orthogonal views without knowing which individual on one scene corresponded to the same individual in the other view. By mapping the trajectories of each nauplius and determining their coordinates, the movements in the  $x, z$  plane could be compared to movements in the  $y, z$  plane. Individuals can be identified by matching the temporal and spatial sequence of movements in the  $z$ -axis. Three-dimensional data were used to estimate modal nearest-neighbor distance (NND) within the swarms (Leising & Yen, submitted).

#### *Swarm formation models*

The curve describing the rate of aggregation was modeled by logistic versus saturation curves. A good fit to the logistic curve would indicate that the rate of aggregation is enhanced by the presence of other swarming individuals, implying that mutual communication was accelerating the rate of aggregation (Okubo & Anderson 1984). The equation for the logistic model is:

$$N = \frac{N_0 K e^r}{N_0 K e^r - (N_0 - K)} \quad (10.1)$$

where  $N$  is the number of individuals,  $N_0$  is the initial swarm size, here designated as 1, and  $K$  is the maximum number in the swarm. The variable  $r$  describes the rate of approach to the maximum.

Swarm formation also can be modeled with the saturation curve where individuals are attracted independently to the swarm marker (Okubo & Anderson 1984). Therefore, in this model, swarm formation is not dependent on mutual communication. The saturation curve is expressed by the equation:

$$N = K(1 - e^{-bt}) \quad (10.2)$$

where  $N$  is the number of individuals within the swarm,  $K$  is the maximum number in the swarm or swarm size, and  $b$  describes the rate of approach to the maximum. Without communication, swarming members may orient themselves only to the attractant. On the other hand, interacting swarm members may show some attraction or orientation to other members as well as the attractant, and may alter their swimming patterns accordingly.

The data were fit to the curves using the software package SigmaPlot which estimates the curve's parameters through multiple iterations. The maximum

number aggregated around the light was determined from the SigmaPlot fit of the saturation model to data from 0 to 600 sec for the naupliar stages and from 0 to 60 sec for the copepodid and adult stages. The time needed for 90% of the maximum in the swarm to aggregate ( $T_{90agg}$ ) was determined by solving the derived equation of the saturation model for 90% of the maximum value. Although swarm size differed for each stage, the number of copepods available to swarm was kept constant at 50 individuals. The data from 600 sec (light off) to 840 sec was fit to a second-order polynomial, and the time until 90% of the maximum number in the swarm was dispersed ( $T_{90dis}$ ) also was determined by solving the derived equation. These time measures,  $T_{90agg}$  and  $T_{90dis}$ , help quantify attractive versus repulsive forces.

#### Fractal analysis of trajectories

A fractal dimension ( $D$ ), first introduced by Mandelbrot (1977, 1983), was applied by Dicke and Burrough (1988) and Sugihara and May (1990) to describe the complexity of a trajectory, where  $D$  represents a measure of roughness or irregularity. Dicke and Burrough (1988) used the estimated  $D$  value as a quantitative discriminator to compare tortuosity of various insect trails. Here we estimate  $D$  to describe trajectories taken by individual zooplankters.  $D$  values are

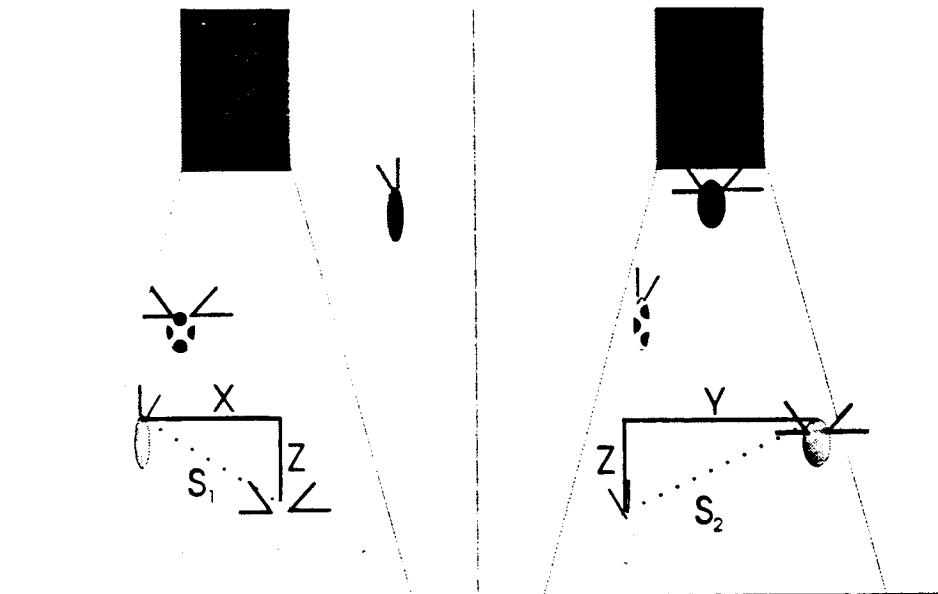


Figure 10.2. Hypothetical distribution of 4 nauplii ( $\gg\ll$ ) beneath a light source, portrayed in an  $x,z$  and  $y,z$  projection (designed by David M. Fields). Patterns on body show identity of nauplii, permitting matching. Distances ( $s_1, s_2$ ) are shown between matched nauplii in two projections.

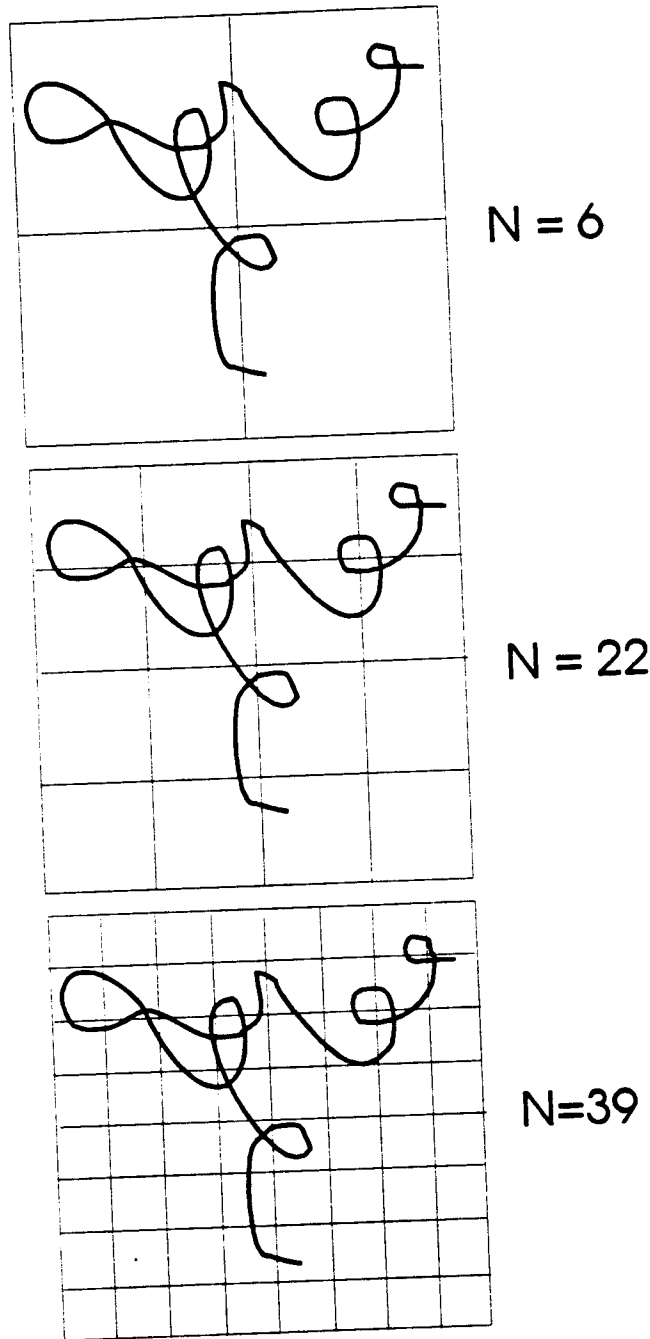


Figure 10.3. Superimposition of squares of smaller and smaller side lengths ( $R$ ) used to estimate the fractal dimension of a trajectory taken by a late nauplius of *Coullana canadensis* as it approached a point light source.  $N$  is the number of squares that the trajectory intersected.



compared across different stages as well as at different times in the evolution and maintenance of a swarm. Paired trajectories were mapped out for each 90 degree view and analyzed individually by the "dividers" method of varying step size (Dicke & Burrough 1988; Sugihara & May 1990). Acetate tracings were taken of the paths off a 30-cm videomonitor. The path was divided into two sectors corresponding to (1) directed swimming to the light and (2) swarming behavior under the light. A single square (4.6 cm  $\times$  4.6 cm) was positioned so as to enclose as much of the trajectory as possible *under* the light (i.e. within the swarm) versus the path taken *to* the light. The square was subdivided four times to provide the values of  $R$  (length of side;  $R = 2., 1.15, 0.575, \text{ and } 0.288$  cm, respectively) and  $N$  (number of squares that a trajectory intersected; Fig. 10.3). The fractal dimension ( $D$ ) was computed as the slope of  $\ln R$  vs.  $\ln N$ . A  $t$ -test (Sokal & Rohlf 1981) was performed to ascertain differences in mean values. In a two-dimensional view, fractal dimensions can range from 1.0 (straight line) to 2.0 (maximum tortuosity).

### 10.3 Results

All stages of *Coullana canadensis* were attracted to the light. Copepods showed directed swimming, resulting in a clumped distribution centered around the light. Soon after the light was illuminated, many animals came into the field of view surrounding the light. When the light was extinguished, the copepods resumed a more random-walk pattern of movement resulting in an even redistribution throughout the tank. Different developmental stages showed different dynamics of patch formation (Fig. 10.4). Swarms of late nauplii were denser (53% of the number in the tank) than those formed by the early nauplii (24%). Although copepodids and adults initially were attracted to the light, after 2 min of illumination no more than 20% of the copepodids and 10% of the adults remained up in the water column. The two models used to describe the rate of swarm formation, the logistic and saturation curves, fit the empirical data equally well for the naupliar stages (Fig. 10.5; Table 10.1). The rate of aggregation during the exponential phase of swarm formation, compared as  $T_{90agg}$ , was significantly shorter for the late nauplii ( $39 \pm 7.1$  sec,  $n = 2$ ) than the earlier nauplii ( $84 \pm 25.4$  sec,  $n = 2$ ). However, there was no significant difference in the swarm dispersal time ( $T_{90dis}$ ).

Analyses of the multiple exposures (Fig. 10.6A,B) of the swarms during the plateau phase showed that the shape of the swarm appeared conical below the light source. In the 50-individual treatment, a swarm of 12 nauplii formed. Swarm density declined exponentially away from the source ( $-0.32, r^2 = 0.956$ ). The border enclosing 95% of the swarm was 3.7 mm. In the 200-individual treat-

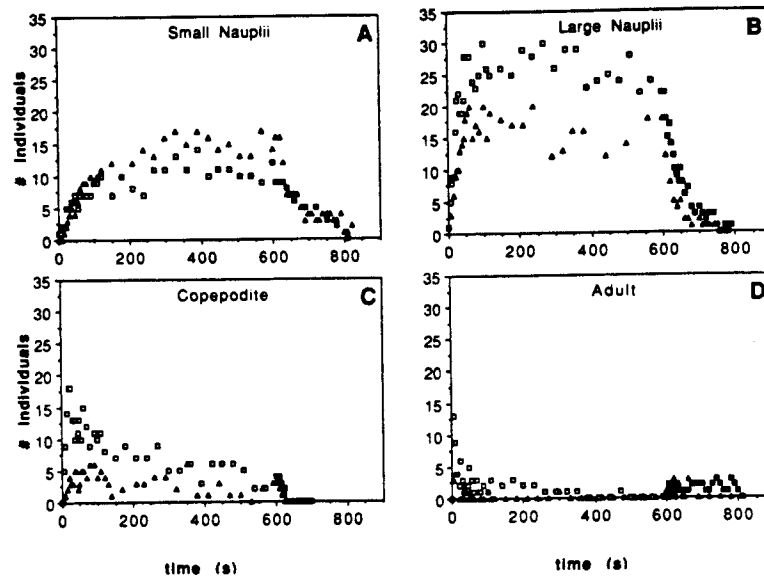


Figure 10.4. Aggregation of four developmental stages of *Coullana canadensis* around a 2-mm-diameter fiber optics light source. Each panel shows the number of animals gathering at the light source over time (seconds) for early nauplii (A), later nauplii (B), early copepodids (C), and adults (D). The light was illuminated at 0 sec (open symbols) and extinguished at 600 sec (closed symbols). Trials (I squares, II triangles), separated by 3–7 days, represent two responses to the same light source for a different group of each stage. The total number of animals within 100-ml tank was 50.

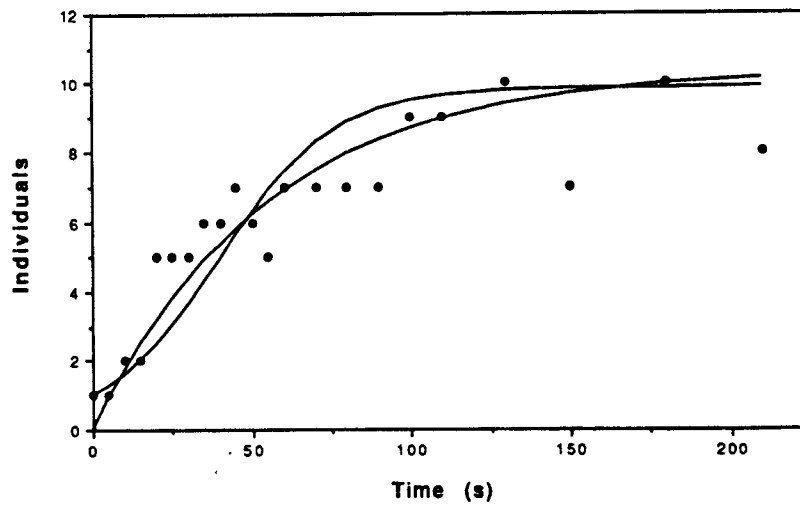


Figure 10.5. Rate of aggregation as modeled by the logistic (S-shaped curve) and saturation (smooth rise) equations when 50 nauplii *Coullana canadensis* were added to the tank and were available for patch formation. Parameters for the best fit curves to these models are listed in Table 10.1.

Table 10.1. Parameters describing the best-fit of the saturation and logistic equations modeling the aggregation dynamics of two developmental stages of *Coullana canadensis*: early nauplii (EN) and late nauplii (LN);  
n = sample size

Stage (n)	Saturation			Logistic		
	K	b	res	K	r	res
EN (50)	10.30	0.018	35.235	9.86	0.055	41.986
EN (50)	5.82	0.033	67.490	5.91	0.063	65.787
EN (200)	59.93	0.017	131.792	56.82	0.090	172.712
LN (50)	26.36	0.046	74.644	25.62	0.175	75.159
LN (50)	14.98	0.039	61.702	14.60	0.127	60.372

ment, a 64-member swarm formed ( $-0.28$ ;  $r^2 = 0.916$ ; 95% at 4.5 mm). The patch size/density analysis showed that nearest-neighbor distance (NND) varied with distance from the light source as well as with swarm population size. Preliminary estimates of nearest-neighbor distances of an 18-member swarm showed that there was approximately a 1–2 body length separation between swarming nauplii. Modal values for center-to-center distances were 0.517, 0.625, and 0.603 mm (Leising and Yen submitted).

All developmental stages of *C. canadensis* showed directed swimming, indicating positive phototaxis. For all stages, the fractal dimension for the path taken to the light was nearly straight (Fig. 10.7; Table 10.2). Both copepodids and adults swarm toward the light in an undulating fashion. However, upon reaching it, these stages would stop swimming and sink. In contrast, when the nauplii were within 2 mm of the light, the spiral became tighter and the net displacement decreased (Fig. 10.7). Within the swarm, the mean fractal dimension of the early and late naupliar paths was significantly higher than that for the copepodid and adult stages (an 11% difference,  $P < 0.02$ ; Fig. 10.8, Table 10.2). The higher fractal dimension indicates nauplii were moving around and exploring their swarm volume more completely than either copepodids or adults.

Adults rest longer between swimming bouts and consequently sink farther from the light due to their high sinking speed. Sinking speeds were well correlated with  $T_{90dis}$ , showing that high sinking rates limited swarm formation (Fig. 10.9). Because sinking speed was a function of increasing body length (i.e. age), sinking effectively removed older stages from the area around the light source. Instead of aggregating near the light source like the nauplii, these stages appeared to accumulate within the area on the bottom lit by the cone of light emanating from the light source.

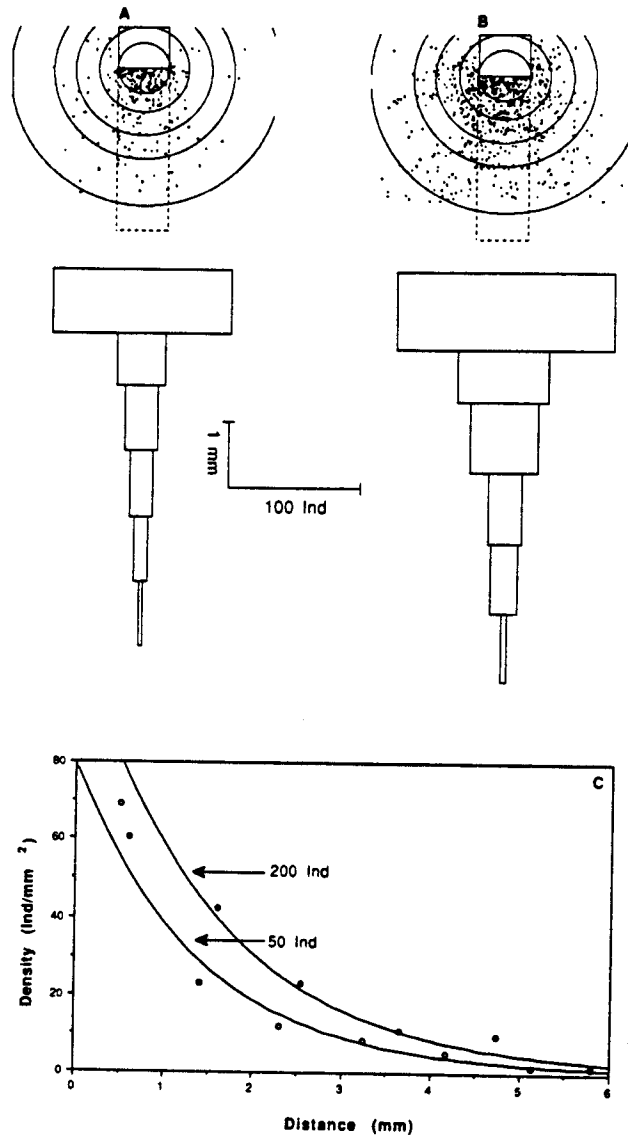


Figure 10.6. Multiple exposures (20 frames) of two-dimensional projections of spatial distribution of *Coullana canadensis* swarms around a fiberoptic light source when 50 early nauplii (A) and 200 early nauplii (B) were available for patch formation. The radii of the concentric circles around the 12-member swarm in A were 1.0, 1.8, 2.8, 3.7, and 5.6 mm. The radii of the concentric circles around the 64-member swarm in B were 1.2, 2.0, 3.1, 4.2, and 6.3 mm. The decline in the number of animals, enumerated in the column under the light source, with distance from the light source is depicted below each swarm illustration. (C) The relationship between distance from the light source vs. the areal density of swarms of two different sizes within a column below the light source.

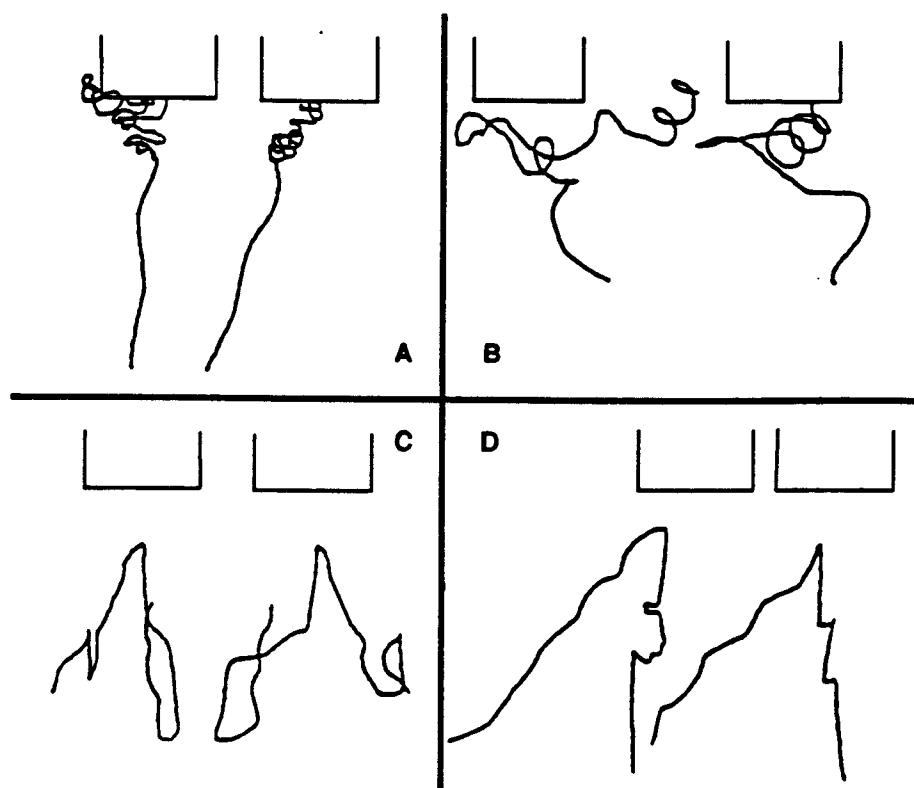


Figure 10.7. Typical two-dimensional trajectories of the developmental stages of *Coullana canadensis* when attracted to the light source (box drawn above paths). Both perpendicular views ( $x,z$ : left side view and  $y,x$ : right side view) are shown for (A) early nauplii, (B) late nauplii, (C) early copepodids, and (D) adults.

## 10.4 Discussion

### 10.4.1 Zooplankton swarms

While aggregative behavior has been well studied in larger aquatic organisms (fish, krill) and terrestrial animals (mammals, birds, insects), little is known about how copepods form aggregations or how they maintain aggregations against the tendency of spreading by random motion or the dispersive energy of mixing in the ocean. Furthermore, we have little quantitative knowledge of the cues leading to aggregation, or of the purpose of these aggregations once formed. The existence of patchiness in zooplankton distributions were once inferred, when the metabolic needs of fish larvae could not be reconciled to the too-low average concentration of their prey in the sea. Laboratory-based behavioral observations also inferred the occurrence of patches in nature because zooplankters entering a created "patch" increased their turning rate, a behavior

Table 10.2. Fractal dimension ( $D \pm 95\%$  confidence interval,  $n$  = number of replicates) of trajectories taken by four developmental stages of *Coullana canadensis* [early nauplii (EN), late nauplii (LN), copepodids (COP), and adults (AD)] in response to illumination of a 2-mm point source of light.  $D_a$  and  $D_b$  are the fractal dimensions of the trajectories from paired orthogonal two-dimensional projections.  $D_s$  are the dimensions for animals swimming under the light within the swarm, while  $D_p$  are the dimensions for animals swimming on the path toward the light when first illuminated.

Stage	$D_a$	$D_b$	$D_s$	$D_p$
EN	1.515	1.426		1.182
	1.759			1.154
	1.427	1.459		
	1.561	1.473		
	1.552	1.310		
LN	1.469	1.416		
	1.417	1.400		1.209
	1.262	1.455		1.241
		1.459 $\pm$ 0.063 (15)		
COP	1.317	1.426		1.158
	1.231			1.370
	1.426	1.420		
AD	1.426			
	1.380	1.325		1.011
	1.274			
	1.270			1.066
		1.349 $\pm$ 0.054 (10)		1.174 $\pm$ 0.091 (8)

which would tend to keep them in a patch. We now know that zooplankton swarming occurs across a variety of temporal and spatial scales. At smaller scales, fist-sized, ephemeral clouds of *Acartia* form in eddies behind coral heads (Omori & Hamner 1982) or are found milling around shafts of light (Ambler et al. 1991). In contrast, zooplankton can also form extensive layers existing at depth (Alldredge et al. 1984) or migrating as deep-scattering layers (Greene et al. 1991). When swarms were documented by visual or acoustic observations, or chemical probes, the degree of variance in plankton abundance was extremely high relative to the statistical average. These high concentrations were real (Greene & Wiebe Ch. 4) and it is to these larger signals, greater than the noise, that the zooplankton were responding. Here we present a study where we are beginning to examine, not the statistical average concentration per volume, but the aggregated patchy distribution of zooplankton embodied as swarms.

Copepod swarm formation, artificially stimulated in a laboratory setting, permits quantitative analyses of swarm mechanics at both the individual and group level. Temporal analyses showed the evolution and decay of the swarm in

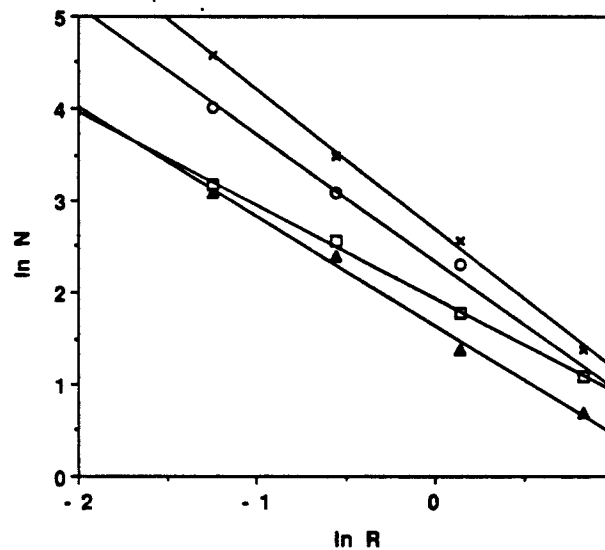


Figure 10.8. Fractal dimensions ( $D$ ) were determined for each two-dimensional trajectory by relating  $N$ , the number of boxes crossed by the path, and  $R$ , the length of the side of the box. The slope (fractal dimension  $D$ ) of  $\ln N$  vs.  $\ln R$  for paths under the light of the early nauplii (x; Fig. 10.7A) and adults (o; Fig. 10.7D) was 1.515 and 1.380, respectively. Fractal analysis of the path to the light in Figure 10.7A and D gave dimensions of 1.182 for the early nauplii (closed triangles) and 1.011 for adults (open boxes).

response to the presence of a light source. Light could easily be replaced by another modality, such as a chemical attractant. Thus, the laboratory-based situation can be used to characterize the dynamics of the lifetime of an aggregated swarm in the face of naturally occurring attractive or dispersive forces. An understanding of patch dynamics in small-scale situations such as ours may provide a link from observations of individual zooplankton behavior to the larger patterns observed in open-water zooplankton populations.

#### 10.4.2 Trajectory analysis

A useful way to quantify the shape of a trajectory is by determining its fractal dimension (Dicke & Burrough 1988; Sugihara & May 1990). When fractal values from paired, two-dimensional projections of the same event are equal, the three-dimensional value can be estimated as the two-dimensional value plus one. Fractal dimensions close to 3 describe trajectories that use the entire three-dimensional space. Fractal dimensions close to 2 describe paths that remain within a plane. For example, ants explore flat surfaces and have fractal dimensions close to 2. The three-dimensional fractal value of approximately 2.5 for the nauplii in a swarm is suitable for a pelagic larva balancing full utilization of its

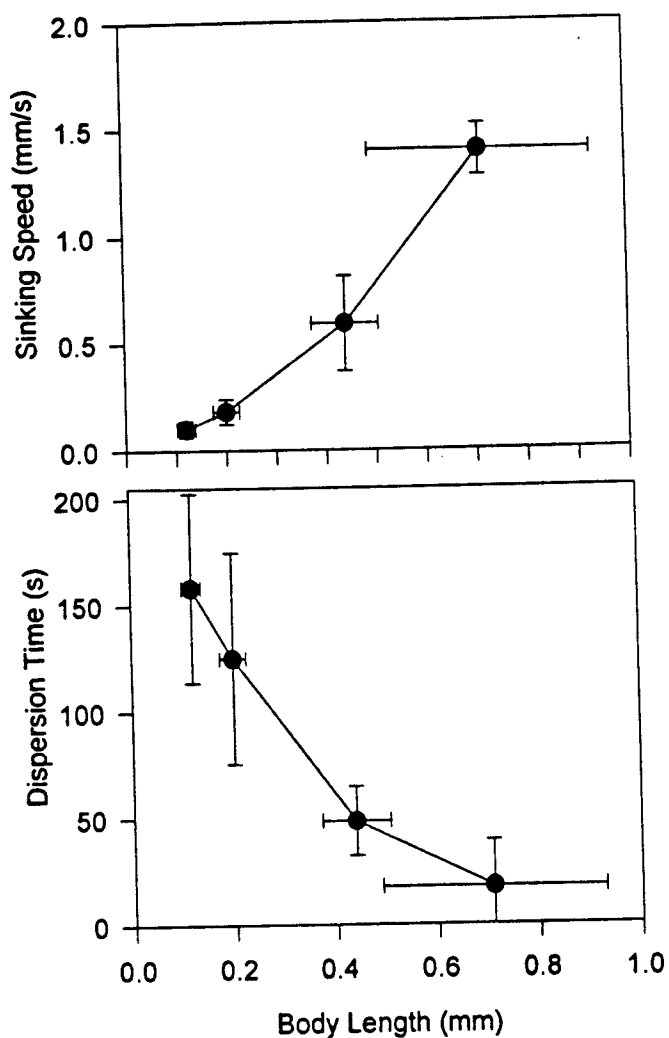


Figure 10.9. Relationship between the (a) time until 90% dispersion ( $T_{90dis}$ ) and (b) sinking speed vs. body length of the four developmental stages of *Coullana canadensis*. The mean  $\pm$  standard deviations are plotted.

three-dimensional space with crowding by swarm mates. The lower fractal dimension of path trajectories during swarm formation indicates that plankters must change their behavioral responses as they approach external attractants (e.g. light source), sense increasing swarm density, or both. Fractal analysis can provide a measure to compare paths taken by unpolarized animals or paths taken during the different phases (evolution, maintenance, decay) of swarming. Although swarming may seem to be uncoordinated at the interindividual level



(i.e. high variance in nearest-neighbor distances), the use of fractal analysis can reveal how individual, and individualized, path shapes contribute to the maintenance of the swarm as a whole.

#### 10.4.3 Communication

Once in a swarm, do zooplankton communicate with each other? Communication does not appear to occur by a rapid means of signal transmission, such as visual or sound transmission, because in zooplankton the sense of sight is not acute (Eloffson 1966) and acoustical detection has not been adequately documented (Schröder 1960). Hence, it is unlikely that aggregation can impart protection from predators for zooplankton by more rapid detection and visually mediated response at the level of the group. There must be other, stronger benefits that led to swarm formation in zooplankton, such as facilitation of mating (Brandl & Fernando 1971; Hebert et al. 1980; Gendron 1992) or foraging (Hamner et al. 1983; Kils 1993). Kils (1993) demonstrated how water is moved within swarms of swimming tintinnids (a process known as bioconvection), where surface water, containing concentrated interfacial material, can be entrained to deeper layers while nutrient-rich deeper water can be mixed toward the surface. Besides promoting water mixing, which exposes plankters to more food, bioconvection in a still region of no pycnocline and little turbulence can enhance encounter rate with food particles.

If communication occurs via chemical or mechanical cues which are more slowly transmitted along paths of fluid flow, how do zooplankton respond to each other within a swarm? Rheotactically, krill sense and follow the wake of their school mates (Hamner et al. 1983). The movements of krill schools appear amoeboid, indicating this type of transmission is rather slow (Hamner et al. 1983). Sex pheromones excreted by swimmers present in high numerical abundance within a limited volume may reach threshold concentrations within a swarm, triggering mating. Chemicals exuded from the food or by-products of the foragers' ingestion process can be excreted within a small volume so that concentrations reach thresholds that release behavioral responses such as increased turning frequency or more directed swimming. The ratio of exudates (attractants) to metabolites (deterrents) may determine attraction or dispersion. However, it is important to note that the time needed to observe these responses to chemical cues or fluid mechanical signals is much greater than that needed to see a fish school scatter from a shark or a bird flock swerve around a tree.

In this study, swarm formation by nauplii fit both the logistic and the saturation models equally well. Therefore, any degree of communication between

swarming individuals could not be discerned mathematically. It is unclear to what degree each nauplius responded individually to the light versus the increased presence of neighbors, as both processes lead to swarm formation.

#### 10.4.4 Orientation and arrangement

In fish schools, polarity exists, and there may be set nearest-neighbor distances given certain circumstances. At the level of the group, there is cohesion and edges. In contrast, zooplankton within swarms show seemingly chaotic movement and have no readily apparent orientation or predictable trajectory. Individuals in a plankton swarm are at random angles to one another. No polarity exists and the distance between individuals may be highly variable. Nevertheless, at the level of the group, one can still observe some of the same resultant properties as fish schools display (e.g. cohesion and edges).

What mechanisms or cues allow individual plankters to form a recognizable unit observed as a swarm? It is unlikely that visual perception of swarm mates is a strong orientational cue since few copepods have image-forming eyes. The only copepods that appear to form aggregates that exhibit coordinated movements between individuals, similar to true schooling, are copepods that have lenses in front of their photoreceptor (*Labidocera pavo* – Ueda et al. 1983); yet these lenses are not attached to focusing muscles nor is there any evidence of an image-forming retina within the photoreceptor. The general lack of image-forming visual perception of swarming copepods may preclude an ability to orient to each other with linearly symmetrical spacing patterns, or to respond with quick cross-school synchrony (Hamner et al. 1983).

It is entirely likely that swarming cues in zooplankton are nonvisual. We know relatively little about the spatial distribution of chemical or fluid mechanical cues within a swarm. These patterns are difficult to visualize and to document in time and space and, hence, are not familiar. For an animal that has no eyes and is chemoreceptive, orientation may be along trails of high chemical concentration (Hamner & Hamner 1977; Poulet & Ouellet 1982). Mechanoreceptive plankters may align along gradients of minimum shear (Yen & Fields 1992) or minimum change in pressure. Local orientation in zooplankton may be along streamlines generated in the flow field surrounding swimming or feeding neighbors. Neither chemical trails nor turbulence follow necessarily regular spatial patterns in three-dimensional space that would result in zooplankter orientation with the familiar spacing of bird flocks or fish schools. Thus, the spatial distribution and movement patterns exhibited by swarming zooplankton may reflect the three-dimensional spatial distribution of the signals in the sea which they sense.

#### 10.4.5 Spacing and perceptive field

The definition of interindividual distance, and thus the density of the patch, may be related to an individual's maximum perceptive distance. Vision, chemoreception, and mechanoreception each have different perspective ranges for copepods, making them variously important at different spatial scales and reaction times. Nearest neighbors may be separated by the span of the appropriate sensor. For example, individuals may remain separated from each other by a distance determined by the sensitivity of a mechanoreceptor and the intensity of a hydrodynamic signal emanating from a neighbor (Leising & Yen, ms.). The three-dimensional pattern of signal transmission also will influence the paths and positions taken by members within the swarm. Individual plankters, unable to sense beyond the limits of their perceptive range, could be coordinated in a loose form of sensory integration (see Schilt & Norris Ch. 15, for an extended discussion of the sensory integration phenomenon), each sensing and responding to their closest neighbor. Few measurements of these gradients have been taken along with the orientation by the animals.

### 10.5 Conclusions

For small organisms like zooplankton dispersed in a huge ocean, it is fortunate that aggregations form – so that predators can find their prey and reproductively mature plankters can find their mates. Zooplankton, considered at the mercy of ocean currents, indeed can execute directed movements of their own. Such movements include attack lunges, escape flights, and mate tracking. These *individual* moves give evidence that zooplankton are not passive, but rather are active – responding to signals transmitted through the fluid medium, the sea. Even though we certainly need a greater understanding of the attractive cues that elicit *group* responses from zooplankton populations and how such forces maintain the swarm in spite of constant dispersive action, it is documented clearly that zooplankton swarms exist and show many of the properties of vertebrate congregations. Here we presented a means to begin a quantitative analysis of swarming behavior: swarm size, path structure, rates of evolution and decay of aggregations. Future research, nesting the 3-D flow visualization optical design within an in situ sonified volume, could provide the data for ground-truthing acoustic images. Overlaying maps of 3-D paths taken by acoustic images of swarm members onto dynamic fluid structures can verify our consideration that the zooplankton tracks can reveal aspects of the structure of fluids at small temporal and spatial scales.

### **Acknowledgments**

We would like to thank Julia Parrish and Bill Hamner for organizing the 3-D aggregation meeting at Monterey Bay Aquarium, for putting this book together, and for insightful criticism of this chapter. We would like to thank Akira Okubo for his enthusiasm and expert guidance in many aspects of this study. We would like to thank David M. Fields for statistical and technical assistance, Andrew W. Leising for contributing his unpublished estimates of NND, and Darcy Lonsdale for providing cultures of *C. canadensis*. J. Yen would like to thank Claudia Mills for the opportunity to participate in Pisces IV dives in Saanich Inlet, Canada, where she saw that copepods did swarm in dense patches and layers. We thank the Ward Meville Foundation for providing a summer undergraduate student fellowship to E. A. Bundock. This research also was supported by the Office of Naval Research contract N-00014-92-J-1690 and National Science Foundation grant OCE-8917167 and OCE-9314934 to J. Yen. This is Contribution No. 1050 from the Marine Sciences Research Center at the State University of New York at Stony Brook.



# ANIMAL GROUPS IN THREE DIMENSIONS

Edited by  
**Julia K. Parrish and William M. Hamner**

This book is about the ways in which many animals form groups, for instance, schools of fish, flocks of birds, and swarms of insects. Covering both invertebrate and vertebrate species, the authors investigate three-dimensional animal aggregations from a variety of disciplines, from physics to mathematics to biology.

Each of the four main sections of the book has an introductory chapter that lays the framework for subsequent chapters. The first section is devoted to the various methods, mainly optical and acoustic, used to collect three-dimensional data over time. The second section focuses on analytical methods used to quantify pattern, group kinetics, and interindividual interactions within the group. The section on behavioral ecology and evolution deals with the functions of aggregative behavior from the point of view of an inherently selfish individual member. The final section presents an alternative to the empirical study of animal aggregation, namely the use of models to elucidate how group dynamics at the individual level creates emergent patterns at the level of the group.

In keeping with the interdisciplinary nature of the subject, the book is designed to allow the reader to jump across chapters, and even across sections, without a loss of continuity.

Researchers interested in behavioral ecology or modeling biological systems would benefit from reading this book.

**CAMBRIDGE**  
UNIVERSITY PRESS

ISBN 0-521-46024-7



9 780521 460248

Cover photograph: Migrating shore birds; Gray's Harbor, Washington © Art Wolfe, 1997, used with permission.

Cover design by Brian H. Crede/bc graphics